Acta Crystallographica Section D
Biological Crystallography
ISSN 0907-4449

Crystallization and preliminary X-ray crystallographic studies of the small form of glucose-inhibited division protein A from *Thermus thermophilus* HB8

Wakana Iwasaki,[a] Hideyuki Miyatake,[a] Akio Ebihara[a] and Kunio Miki[a,b]*

[a]RIKEN Harima Institute/SPring-8, Koto 1-1-1, Mikazuki-cho, Sayo-gun, Hyogo 679-5148, Japan, and [b]Department of Chemistry, Graduate School of Science, Kyoto University, Sakyo-ku, Kyoto 606-8502, Japan

Correspondence e-mail: miki@kuchem.kyoto-u.ac.jp

Received 17 October 2003
Accepted 9 January 2004

Glucose-inhibited division protein A (GidA) acts in tRNA modification. It has been suggested that GidA is involved in the biosynthesis of the hypermodified nucleotide 5-methylaminomethyl-2-thiouridine in the wobble position of bacterial tRNAs, which stabilizes codon–anticodon interactions. *Thermus thermophilus* HB8 has a putative small *gidA* gene in addition to the normal *gidA* gene. The crystallization and preliminary X-ray crystallographic studies of the product of this small *gidA* gene ($GidA_{small}$) are reported here. The crystals belong to space group $P3_121$ or $P3_221$, with unit-cell parameters $a = b = 78.51$, $c = 66.10$ Å and one monomer per asymmetric unit. The crystals were found to diffract X-rays to beyond 1.65 Å resolution.

1. Introduction

The gene for glucose-inhibited division protein A (*gidA*) was first isolated in association with a glucose-inhibited division phenotype of *Escherichia coli* (von Meyenburg & Hansen, 1980). The *gidA* genes are well conserved among a wide range of prokaryotes and are generally localized near the chromosomal replication origin. GidA is therefore proposed to play a role in control of cell division. However, GidA has recently been shown to be involved in the biosynthesis of the hypermodified nucleotide 5-methylaminomethyl-2-thiouridine (mnm^5s^2U34; Björk, 1996; Brégeon *et al.*, 2001), which is found in the wobble position of bacterial tRNAs specific for glutamate, lysine, glutamine, arginine and leucine (Björk, 1996). This modification is necessary to stabilize codon–anticodon interactions (Brégeon *et al.*, 2001). The precise role of GidA in the modification pathway is unknown. Humans and yeast have the GidA homologue Mto1, which is thought to play a role in mitochondrial tRNA modification (Colby *et al.*, 1998; Li *et al.*, 2002). GidA binds FAD (White *et al.*, 2001), but it remains unknown whether GidA catalyses oxidation–reduction reactions.

A subset of organisms have a second smaller GidA. *Thermus thermophilus* HB8 has a putative small *gidA* gene in addition to the normal *gidA* gene. The gene product of the small *gidA* ($GidA_{small}$) consists of 232 amino acids, while that of the conventional *gidA* consists of 597 amino acids. Fig. 1 shows the amino-acid sequences of GidA and $GidA_{small}$ of *T. thermophilus* HB8. Neither the crystal structure of GidA nor $GidA_{small}$ have been reported. To provide structural insight into the function of GidA, we have initiated crystallographic studies of $GidA_{small}$. Here, we report the crystallization and preliminary X-ray diffraction analysis.

2. Materials and methods

2.1. Expression and purification

The $gidA_{small}$ gene was amplified from *T. thermophilus* HB8 genomic DNA by PCR using the following oligonucleotide primers containing artificial *Nde*I and *Bgl*II sites (in bold): 5′-ATAT**CATATG**GCGGCGTACCA-GGTCCTCATCGTGGGGG-3′ and 5′-ATAT-**AGATCT**TTATTACCCAAGCTCATGGAG-AAGGTGCTCC-3′. The PCR product was subcloned into pT7Blue (Novagen) by TA cloning. The plasmid was digested with *Nde*I and *Bgl*II and was ligated into the *Nde*I and *Bam*HI sites of bacterial expression vector pET11a (Novagen), in which the $gidA_{small}$ gene is under control of the T7 promoter. This recombinant plasmid was then transformed into *E. coli* strain BL21 (DE3). The transformed bacteria were grown overnight at 310 K with shaking in Miller LB broth containing ampicillin (50 μg ml^{-1}). The cells were harvested and sonicated in 20 m*M* Tris–HCl buffer pH 8.0 containing 50 m*M* NaCl. The crude extract was incubated at 343 K for 10 min, cooled on ice and ultracentrifuged at 65 300*g* for 60 min. Ammonium sulfate was added to the supernatant to a final concentration of 1.5 *M*. The solution was then loaded onto a Resource ISO column (Amersham Bioscience) equilibrated with 50 m*M* sodium phosphate buffer pH 7.0 containing 1.5 *M* ammonium sulfate and eluted with a linear gradient of ammonium sulfate. The fractions containing $GidA_{small}$ were desalted using a HiPrep 26/10 desalting column (Amersham

Bioscience) and applied onto a Resource Q column (Amersham Bioscience) equilibrated with 20 m*M* Tris–HCl buffer pH 8.0. $GidA_{small}$ was eluted with a linear gradient of NaCl. Fractions containing $GidA_{small}$ were pooled and concentrated by ultrafiltration. The concentrated solution was eluted through a HiLoad 16/60 Superdex 75 pg column (Amersham Bioscience) equilibrated with 20 m*M* Tris–HCl pH 8.0 containing 150 m*M* NaCl. The fractions containing $GidA_{small}$ were concentrated to 7.2 mg ml^{-1} by ultrafiltration in solutions of 20 m*M* Tris–HCl buffer pH 8.0 containing 1 m*M* dithiothreitol. The final preparation appeared as a single band after SDS–PAGE and was stored at 277 K.

2.2. Dynamic light-scattering studies

Prior to the experiment, the protein samples were filtered with disposable 0.02 µm pore-size Anotop-10 inorganic membrane filters (Whatman). The dynamic light-scattering characteristics of the protein solution were analysed using a DynaPro-99-E50 molecular-sizing detector (Protein Solutions) at 293 K. Data were analysed using the *DYNAMICS* software (Protein Solutions).

2.3. Crystallization

Crystallization conditions were initially screened with the sitting-drop vapour-diffusion method using Hampton Research Crystal Screen I and Cryo at 293 K. Sitting drops were prepared by mixing 1 µl protein solution (7.4 mg ml^{-1} in 20 m*M* Tris–HCl pH 8.0, 1 m*M* DTT) with 1 µl reservoir solution on a microbridge (Hampton Research). The 2 µl sitting drops were then equilibrated with 500 µl of reservoir solution at 293 K.

2.4. Data collection

Prior to data collection, crystals were soaked for a few seconds in a mother liquor containing 23% glycerol as cryoprotectant and then mounted in the cryogas stream at 90 K. X-ray data were collected at the synchrotron-radiation source at beamlines BL45XU (Yamamoto *et al.*, 1998, 2001) and BL44B2 (Adachi *et al.*, 1996) at SPring-8 (Harima, Japan). A data set of 360 imaging frames was recorded using a MAR CCD165 detector system at a 115 mm crystal-to-detector distance, with a 1° oscillation angle and a 5 s exposure time per imaging frame. All data were processed and reduced using the *HKL*2000 package (Otwinowski & Minor, 1997) and the *CCP*4 software suite (Collaborative Computational Project, Number 4, 1994).

2.5. Heavy-atom derivative search

More than ten different metal reagents at concentrations of 0.1–10 m*M* and Xe gas were used in the heavy-atom derivative search.

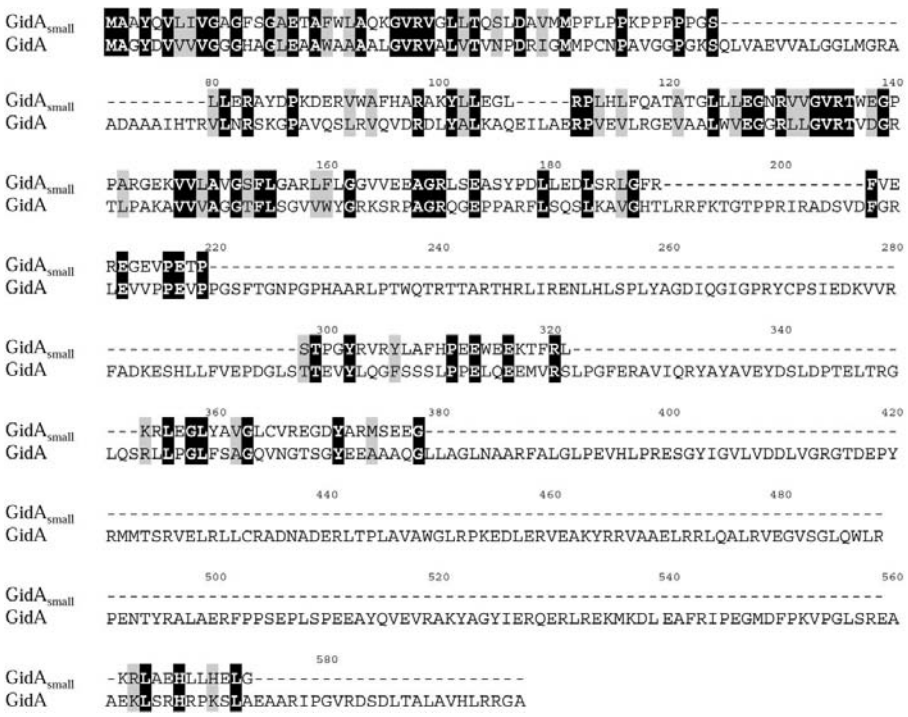

Figure 1
Sequence alignment of GidA and $GidA_{small}$ from *T. thermophilus* HB8. Identical and conservative residues are shaded black or grey, respectively.

3. Results

It is known that GidA binds FAD (White *et al.*, 2001). The purified $GidA_{small}$ was yellow in colour and showed absorbance from 370 to 500 nm, with peaks at 388 and 453 nm. Dynamic light-scattering results indicated the protein to be monodisperse and to have a hydrodynamic radius of 2.4 nm and an apparent molecular weight of 25 kDa, suggesting that $GidA_{small}$ exists as a monomer in solution.

Crystal Screen I (Hampton Research) condition No. 6 (30% PEG 4000, 0.1 *M* Tris–HCl pH 8.5, 0.2 *M* $MgCl_2$) yielded small rod-shaped crystals within a few days. After refining the condition, crystals suitable for

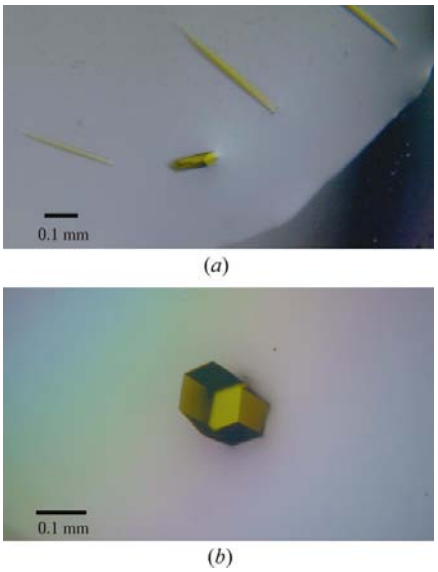

Figure 2
A crystal of $GidA_{small}$. (*a*) Rod-shaped crystals grown under PEG 4000 conditions. The crystal has approximate dimensions of 0.05 × 0.05 × 0.5 mm. (*b*) A hexagonal prismatic crystal grown under magnesium formate conditions, with approximate dimensions of 0.15 × 0.15 × 0.3 mm.

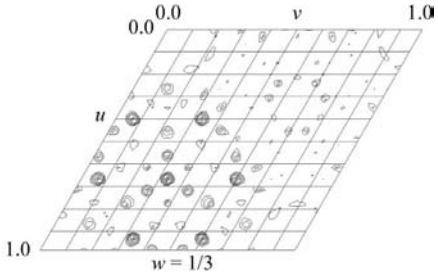

Figure 3
A Harker section (w = 1/3) of the Bijvoet difference Patterson map calculated from peak data in the 15–3.0 Å resolution range. Contours are drawn at 0.5σ levels, starting from 1σ.

Table 1
Data-collection and processing statistics.

Values in parentheses are for the highest-resolution shell. The peak MAD data were collected last among the three wavelengths. The peak data therefore have the lowest resolution as a result of radiation damage.

	Hg derivative (rod-shaped crystal)			
	Low remote	Edge	Peak	Native (prismatic crystal)
Wavelength (Å)	1.0200	1.0086	1.0080	1.0000
Space group	$P3_121$ or $P3_221$			$P3_121$ or $P3_221$
Unit-cell parameters (Å)	a = 78.62, c = 66.11			a = 78.62, c = 66.11
Resolution range (Å)	40.0–2.50 (2.59–2.50)	40.0–2.50 (2.59–2.50)	40.0–2.70 (2.80–2.70)	40.0–1.65 (1.71–1.65)
No. observations	151287	105970	113425	1120529
No. unique reflections	15888	8226	6741	28463
$R_{\rm merge}$† (%)	9.9 (22.9)	9.8 (17.2)	9.5 (18.0)	4.1 (11.3)
Completeness (%)	100 (100)	96.8 (98.0)	99.0 (99.2)	99.1 (91.4)
$\langle I\rangle/\langle\sigma\rangle$	28.5 (10.4)	30.1 (12.6)	32.2 (12.2)	98.2 (22.0)

† $R_{\rm merge} = [\sum_h \sum_i |I_i(h) - \langle I(h)\rangle|/\sum_h \sum_i I_i(h)] \times 100$, where $\langle I(h)\rangle$ is the mean of the $I(h)$ observation of reflection h.

X-ray analysis were obtained with a reservoir solution consisting of 29.7% PEG 4000, 0.31 *M* $MgCl_2$ and 0.1 *M* Tris–HCl pH 7.6 at 293 K (Fig. 2*a*). The crystals diffracted to 1.90 Å. Crystal Screen I condition No. 44 (0.2 *M* magnesium formate) yielded a hexagonal prismatic crystal (Fig. 2*b*) which diffracted X-rays beyond 1.65 Å. The crystal appeared after an incubation period of more than a year and unfortunately was difficult to reproduce. The data-collection statistics are summarized in Table 1. These two types of crystals both belong to trigonal space group $P3_121$ or $P3_221$, with very similar unit-cell parameters. Assuming the presence of one molecule per asymmetric unit, the crystal volume per unit of protein weight is $V_{\rm M}$ = 2.3 Å^3 Da^{-1}, which corresponds to a solvent content of 45.6% (Matthews, 1968). Rod-shaped crystals were used for the heavy-atom derivative search and crystals soaked in 8 m*M* mercury chloride for 3.5 d at 293 K gave interpretable peaks in the Bijvoet difference Patterson map (Fig. 3). For this Hg-derivative crystal, three wavelengths, 1.00750 (peak), 1.00855 (edge) and 1.0200 Å (remote), were selected on the basis of an X-ray absorption spectrum at the Hg $L_{\rm III}$ edge. A structure determination using the MAD strategy based on the Hg-atom position, confirmed and refined with *SOLVE* (Terwilliger & Berendzen, 1999), is currently in progress.

The authors would like to express gratitude to Dr Y. Kawano, Dr H. Naito and Mr H. Nakajima of RIKEN Harima Institute for their kind help in data collection. This work was performed under the 'Structurome' Project of RIKEN Harima Institute and the protein-sample preparation carried out by Professor S. Kuramitsu and his coworkers is greatly appreciated. This work was supported in part by the Special Postdoctoral Researchers Program at RIKEN (to WI) and by a Grant-in-Aid for the Encouragement of Young Scientists from the Ministry of Education, Culture, Sports, Science and Technology of Japan (grant No. 13780491 to WI).

References

Adachi, S., Oguchi, T. & Ueki, T. (1996). *SPring-8 Annual Report*, pp. 230–240. SPring-8, Hyogo, Japan.
Björk, G. R. (1996). In *Escherichia Coli and Salmonella: Cellular and Molecular Biology*, edited by F. C. Neidhardt, R. Curtiss III, J. L. Ingraham, E. C. C. Lin, B. K. Low, B. Magasanik, W. S. Reznikoff, M. Riley, M. Schaechter & H. E. Umbarger, pp. 861–886. Washington DC: American Society for Microbiology.
Brégeon, D., Colot, V., Radman, M. & Taddei, F. (2001). *Genes Dev.* **15**, 2295–2306.
Colby, G., Wu, M. & Tzagoloff, A. (1998). *J. Biol. Chem.* **273**, 27945–27952.
Collaborative Computational Project, Number 4 (1994). *Acta Cryst.* D**50**, 760–763.
Li, X., Li, R., Lin, X. & Guan, M.-X. (2002). *J. Biol. Chem.* **277**, 27256–27264.
Matthews, B. W. (1968). *J. Mol. Biol.* **33**, 491–497.
Meyenburg, K. von & Hansen, F. G. (1980). *Mol. Cell. Biol.* **19**, 137–159.
Otwinowski, Z. & Minor, W. (1997). *Methods Enzymol.* **276**, 307–326.
Terwilliger, T. C. & Berendzen, J. (1999). *Acta Cryst.* D**55**, 849–861.
White, D. J., Merod, R., Thomasson, B. & Hartzell, P. L. (2001). *Mol. Microbiol.* **42**, 503–517.
Yamamoto, M., Kumasaka, T., Fujisawa, T. & Ueki, T. (1998). *J. Synchrotron Rad.* **5**, 222–225.
Yamamoto, M., Kumasaka, T., Yamazaki, H., Sasaki, K., Yokozawa, Y. & Ishikawa, T. (2001). *Nucl. Instrum. Methods Phys. Res. A*, **467**, 1160–1162.